TECHNICAL NOTES

NATIONAL ADVISORY COMMITTEE FOR AERONAUTICS

No. 638

TANK TESTS OF MODEL 36 FLYING-BOAT HULL

By John M. Allison
Langley Memorial Aeronautical Laboratory

Washington
March 1938

NATIONAL ADVISORY COMMITTEE FOR AERONAUTICS

TECHNICAL NOTE NO. 638

TANK TESTS OF MODEL 36 FLYING-BOAT HULL

By John M. Allison

SUMMARY

N.A.C.A. model 36, a hull form with parallel middle body for half the length of the forebody and designed particularly for use with stub wings, was tested according to the general fixed-trim method over the range of practical loads, trims, and speeds. It was also tested free to trim with the center of gravity at two different positions. The results are given in the form of nondimensional coefficients.

The resistance at the hump was exceptionally low but, at high planing speeds, afterbody interference made the performance only mediocre.

INTRODUCTION

Model 36 was designed and built for use in an investigation of the water performance of stub wings. A rather small beam was used, because the stub wings were expected to take part of the load at low speeds. The model was made with a flat deck and the sides of the hull were made parallel forward of the step for half the length of the forebody, in order that the stub wings might be fitted to the sides of the hull by merely squaring the root ends. A hull with parallel sides near amidships has a further advantage from the standpoint of the designer of a transport flying boat because it enables him to maintain the maximum seat and aisle width over the greater portion of the cabin length.

The model was included with several others sent to the propeller-research tunnel for aerodynamic tests. The results of these tests (reference 1) showed that the air resistance throughout a wide range of angles of attack was fairly good, as compared with two other models with flat decks. The hull was not tested with the stub wings attached.

After publication of the wind-tunnel tests, requests for the results of the hydrodynamic tests were received by the Committee. The tests were subsequently made of the hull without the stub wings.

DESCRIPTION OF MODEL

The principal lines of the model are shown in figure 1, and the offsets are given in table I. The model was shaped from a horizontally laminated shell of pine and was finished in gray enamel, wet-sanded and polished to give a smooth surface. Tolerances of ±0.02 inch were held on all offsets below the chine.

The particulars of the model are as follows:

Length:	
Over-all	100.00 in.
To second step	80.00 in.
Forebody	50.00 in.
Maximum beam	14.00 in.
Dead rise at step	20°
Angle of afterbody keel	6-1/4°
Angle of tail extension	10°
Center of moments above keel at step	14.06 in.
Center of moments forward of step	10.00 in.
Depth of main step	0.56 in.
Forebody:	
Percentage of over-all length	50.0
Percentage of length to second step	62.5
Beam:	
Percentage of over-all length	14.0
Percentage of length to second step	17.5
Percentage of forebody length	28.0

Center of moments above keel at step:	
Percentage of over-all length	14.1
Percentage of length to second step	17.6
Percentage of forebody length	28.2
Center of moments forward of step:	
Percentage of over-all length	10.0
Percentage of length to second step	12.5
Percentage of forebody length	20.0
Depth of step, percentage of beam	4.0

The hull has a long straight forebody keel and a chine flare on the forebody only. The angle of afterbody keel and the depth of step are in accordance with N.A.C.A. design practice on somewhat similar forms.

APPARATUS AND METHODS

The N.A.C.A. tank and its original equipment are described in reference 2. The suspension of the model and the method of measuring the trimming moment have since been altered as described in reference 3.

The test program included both general fixed-trim and specific free-to-trim tests. In the general fixed-trim test, the model is towed at constant speed and trim while the load is varied to cover the useful range. Sufficient trims are investigated to determine the minimum resistance at all speeds and the resistance at zero trimming moment at low speeds.

In the specific free-to-trim test, the gross load of the model corresponds to a reasonable gross-load coefficient for a present-day transport flying boat. A calibrated hydrofoil simulates the lift of the wing at a constant angle of attack and is set to make the model leave the water at a speed corresponding to the take-off speed of the assumed flying boat.

The model is balanced about the center of moments so that this point becomes the center of gravity and the trim is influenced only by the water and air forces acting. The trim of the full-size flying boat, however, is affected by aerodynamic moments not simulated in the test set-up.

RESULTS

The nondimensional coefficients used in the presentation of the data are as follows:

Load coefficient, $C_\Delta = \Delta/wb^3$

Resistance coefficient, $C_R = R/wb^3$

Speed coefficient, $C_V = V/\sqrt{gb}$

Draft coefficient, $C_d = d/b$

Rise coefficient, $C_r = r/b$

Trimming-moment coefficient, $C_M = M/wb^4$

where Δ is the load on the water, lb.

w, specific weight of the water, lb./cu. ft. (63.2 for these tests).

b, beam of hull, ft.

R, water resistance, lb.

V, speed, ft./sec.

M, trimming moment, lb.-ft.

g, acceleration of gravity, ft./sec.^{2}

d, draft at main step, ft.

r, rise of the center of gravity of the model, ft.

The data for the fixed-trim test are presented in figures 2 to 7; resistance coefficient C_R, trimming-moment coefficient C_M, and draft coefficient C_d are plotted against speed coefficient C_V with load coefficient C_Δ as a parameter. The center of moments was that shown in figure 1.

The characteristics of the model at best trim were obtained by cross-plotting resistance coefficient and trimming-moment coefficient against trim at selected values of speed coefficient, with load coefficient as a parameter. Minimum resistance coefficient, best trim (trim for minimum resistance), and trimming-moment coefficient at best trim were determined for each speed coefficient. Three of these cross plots are shown in figure 8. Resistance coefficient and trimming-moment coefficient at best trim are plotted in figures 9 and 10, respectively; best trim is plotted against speed coefficient in figure 11.

Resistance coefficient C_R is plotted against C_Δ with C_V as a parameter, in figures 12 and 13 for free to trim and best trim, respectively. The free-to-trim curves of figure 12 are supplemented by a plot of trim against speed coefficient with load coefficient as a parameter for convenience in determining the trim at low speeds. Figures 12 and 13 are useful in making take-off time and distance calculations.

The results of the specific free-to-trim test are presented in nondimensional form in figures 14 and 15. Figure 16 shows the effect upon resistance and trim of moving the center of gravity nearer the step.

Trimming-moment coefficient and draft coefficient at rest are plotted in figures 17 and 18, respectively. These curves are useful in calculating longitudinal stability and in determining water lines of the hull for various static conditions.

DISCUSSION

Resistance characteristics.- The hump resistance of model 36, as determined from the curves of C_R against C_V, based upon best trim (fig. 9) is exceptionally low. The fact that the nondimensional coefficients used were based upon the beam alone makes it difficult to compare fairly the hull forms of quite different length-beam ratio, because the longer hull will have a greater bottom area for a given beam and will therefore be able to carry larger loads at the hump. The resistance at planing speeds is not so favorable as that at the hump, but it compares well with successful American hulls.

A comparison of figure 14 with figure 9 shows that, with the center of gravity 10 inches forward of the step, the hump resistance, free to trim, was about 21 percent higher than that corresponding to best trim and the trim was 2.7° greater than best trim. Trim at high speeds was much too low. The position of the center of gravity was therefore moved 3-1/8 inches aft to a point 6-7/8 inches forward of the step in order to determine the effect on free-to-trim characteristics. Figure 16 shows how the resistance at high speeds was reduced by the change. The hump resistance was, however, almost 40 percent higher than that for best trim, and the trim was 4.3° above best trim. The thrust moment and elevator-control moment would have to be taken into consideration before a final recommendation as to the position of the center of gravity could be made.

Porpoising.- Porpoising was encountered at about 20 feet per second in the tests of the model having the center of gravity 10 inches forward of the step. In order to measure resistance in the porpoising region, it was necessary to apply heavy damping in pitch. With the center of gravity 6-7/8 inches forward of the step, there was but little tendency to porpoise. It should be noted that the model set-up is not dynamically similar to full-scale conditions and any conclusions as to whether or not porpoising will occur at full-scale should be made with caution.

Trimming-moment characteristics.- The curves of trimming-moment coefficient at best trim against speed coefficient (fig. 10) show that, with the hull heavily loaded, large negative moments are produced at low speeds and large positive moments are encountered just above hump speed. At speeds above $C_V = 4.0$, the moments have decreased to such an extent that they may be counteracted with the elevators.

Spray characteristics.- Photographs of the model running free to trim at low speeds are shown in figure 19. In figures 19(a) and 19(b), at a speed just below hump speed, the stern is riding heavily in the water and throwing up a roach. In figures 19(c) and 19(d), at a speed just above hump speed, the pointed afterbody is just touching the water, but the tail extension is clear. Figures 19(e) and 19(f) show the model running at a slightly higher speed; the tail extension and the pointed end of the afterbody are now both clear of the water, and planing of the forebody has been established. The trim shown in the photographs is from 2° to 3° greater than best trim.

Photographs of the model running fixed in trim are shown in figures 20 and 21. Hump conditions with heavy load are shown in figures 20(a) and 20(b). The trim is slightly above best trim. Hump conditions with a smaller load are shown in figures 20(c) and 20(d) with trim slightly under best trim. (See fig. 8.) At the hump, even with a very heavy load, the bow wave is not thrown high enough to be objectionable. In figures 20(e) and 20(f), the model is running near best trim with planing well established. The pictures show water striking the afterbody, indicating that there is some afterbody interference. In figures 21(a) and 21(b), the model is shown running at a higher planing speed. It will be noted by comparing figures 21(b) and 20(f) that afterbody interference is worse at the higher speeds and lighter loads.

Comparison with model 35A.- In figure 22, the load-resistance ratios of models 36 and 35A (reference 4) are compared. Both these models have high length-beam ratios: L/b of model 36 (taking L as the distance from F. P. to the sternpost at the end of the afterbody) is 5.70 and L/b of model 35A is 6.15. Inasmuch as their length-beam ratios are of the same order, the models may be compared fairly on the basis of the nondimensional coefficients based upon beam alon. The load-resistance ratios of figure 22, taken at three speeds, with a wide range in loads, show that model 36 is better at the hump for the heavier loads and model 35A is better in the planing speed ranges. The superiority of model 35A at high speeds is due to the better clearance of the afterbody, especially at light loads.

CONCLUDING REMARKS

The form of model 36 has many of the characteristics favorable for low hump resistance: rather small dead rise; moderate angle of afterbody keel; moderate depth of step; long, straight forebody undersurface; and high length-beam ratio. Several of these features, involving the position of the afterbody with respect to the forebody, affect the resistance at high speed adversely when they improve it at hump speed. Good all-round performance depends upon adjusting the various factors until a satisfactory compromise is reached. Each flying-boat design requires a different compromise. If the total air-plus-water resistance of a contemplated design using the hull form of model 36 gives a critical condition of excess thrust at high speeds with a large amount of excess thrust at hump speed, then the afterbody clearance could be increased to improve high-speed performance at the expense of hump-speed performance.

Model 36, in common with most conventional hulls, has a tendency to trim higher than best trim at the hump, for practical positions of the center of gravity. Unpublished skeleton tests of the model with stub wings show that the stubs act to reduce the trim and the spread between free to trim and best trim. Further tests with various stubs and stub positions are contemplated.

Langley Memorial Aeronautical Laboratory,
National Advisory Committee for Aeronautics,
Langley Field, Va., January 26, 1938.

REFERENCES

1. Hartman, Edwin P.: The Aerodynamic Drag of Flying-Boat Hull Models as Measured in the N.A.C.A. 20-Foot Wind Tunnel - I. T.N. No. 525, N.A.C.A., 1935.

2. Truscott, Starr: The N.A.C.A. Tank - A High-Speed Towing Basin for Testing Models of Seaplane Floats. T.R. No. 470, N.A.C.A., 1933.

3. Allison, John M.: Tank Tests of a Model of the Hull of the Navy PB-1 Flying Boat - N.A.C.A. Model 52. T.N. No. 576, N.A.C.A., 1936.

4. Dawson, John R.: Tank Tests of Three Models of Flying-Boat Hulls of the Pointed-Step Type with Different Angles of Dead Rise - N.A.C.A. Model 35 Series. T.N. No. 551, N.A.C.A., 1936.

TABLE I

Offsets for N.A.C.A. Model 36 Flying-Boat Hull (Inches)

		Distance below base line					Half-breadths				
Station	Distance from F.P.	Keel	Tangency of bottom flare	Main chine	Cove	Upper chine	Tangency of bottom flare	Main chine	Cove	Upper chine	Radius of bottom flare
F.P.	0.00	4.50		4.50				0.15			
1/4	1.25	7.88	5.74	5.49			1.33	1.55			0.69
1/2	2.50	9.12	6.65	6.25			2.08	2.62			1.30
1	5.00	10.65	8.00	7.48			3.13	4.18			2.34
1-1/2	7.50	11.51	8.95	8.41			3.77	5.21			3.13
2	10.00	12.03	9.62	9.12			4.19	5.91			3.73
3	15.00	12.46	10.44	10.05			4.60	6.70			4.49
4	20.00	12.50	10.77	10.47			4.72	6.96			4.87
5 to 10,F	25.00 to 50.00	12.50	10.82	10.56			4.75	7.00			5.00
10,A	50.00	11.94		9.45							
11	55.00	11.39		8.90	7.41	7.41		7.00	7.00	7.00	
12	60.00	10.85		8.50	6.67	6.55		6.60	6.60	6.94	
13	65.00	10.30		8.31	6.15	5.75		5.61	5.61	6.73	
14	70.00	9.75		8.31	5.82	5.02		4.11	4.11	6.31	
15	75.00	9.21		8.44	5.61	4.36		2.26	2.26	5.69	
16,F	80.00	8.66		8.66	5.50	3.78		.15	.15	4.89	
16,A	80.00	5.50									
17	85.00	4.62				3.25				3.93	
18	90.00	3.74				2.76				2.85	
19	95.00	2.86				2.31				1.67	
20	100.00	1.98				1.89				.40	

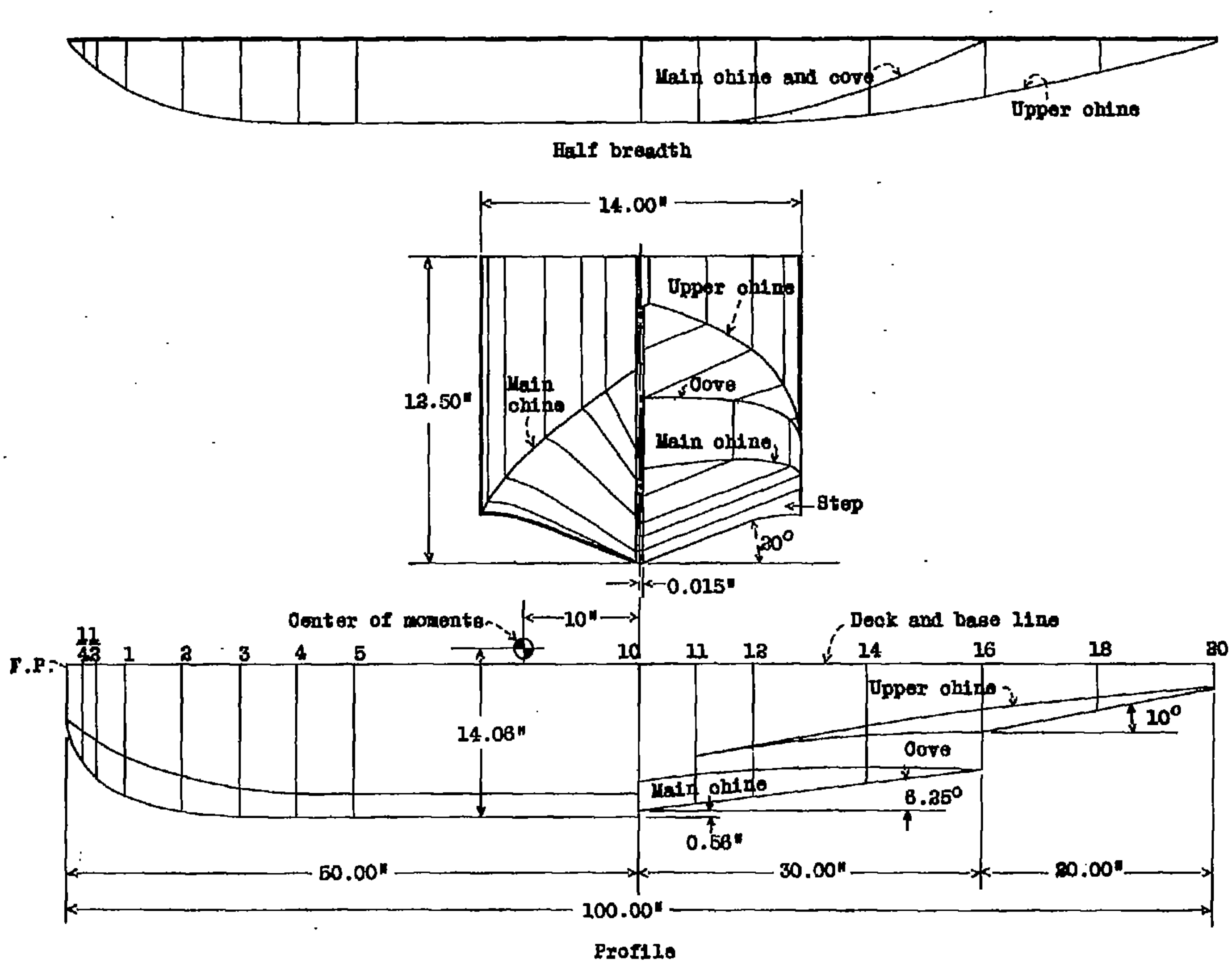

Figure 1. - Model 36. Principal lines and dimensions.

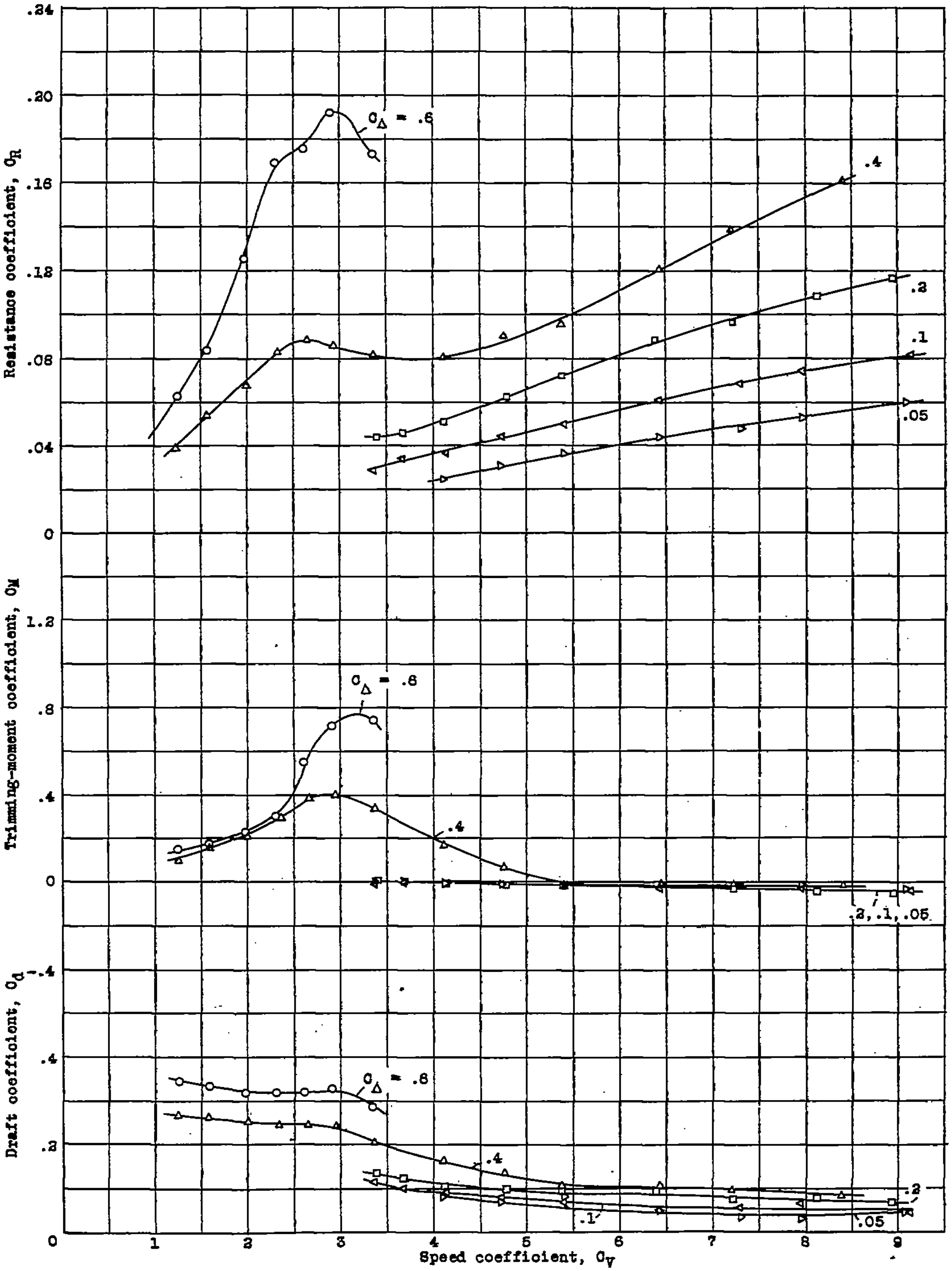

Figure 2. - Model 36. Resistance, trimming-moment, and draft coefficients, $\tau = 3^{\circ}$

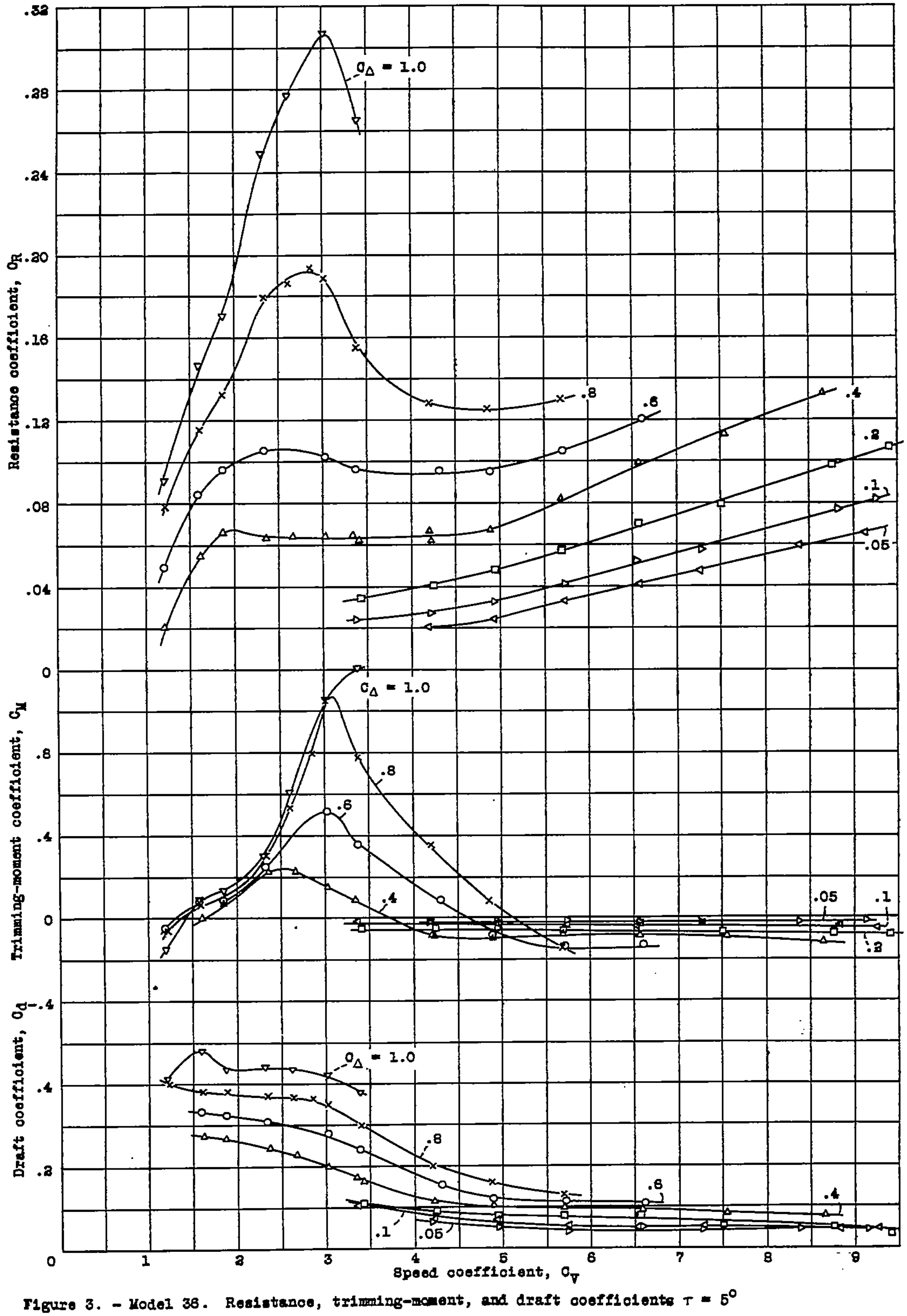

Figure 3. - Model 36. Resistance, trimming-moment, and draft coefficients τ = 5°

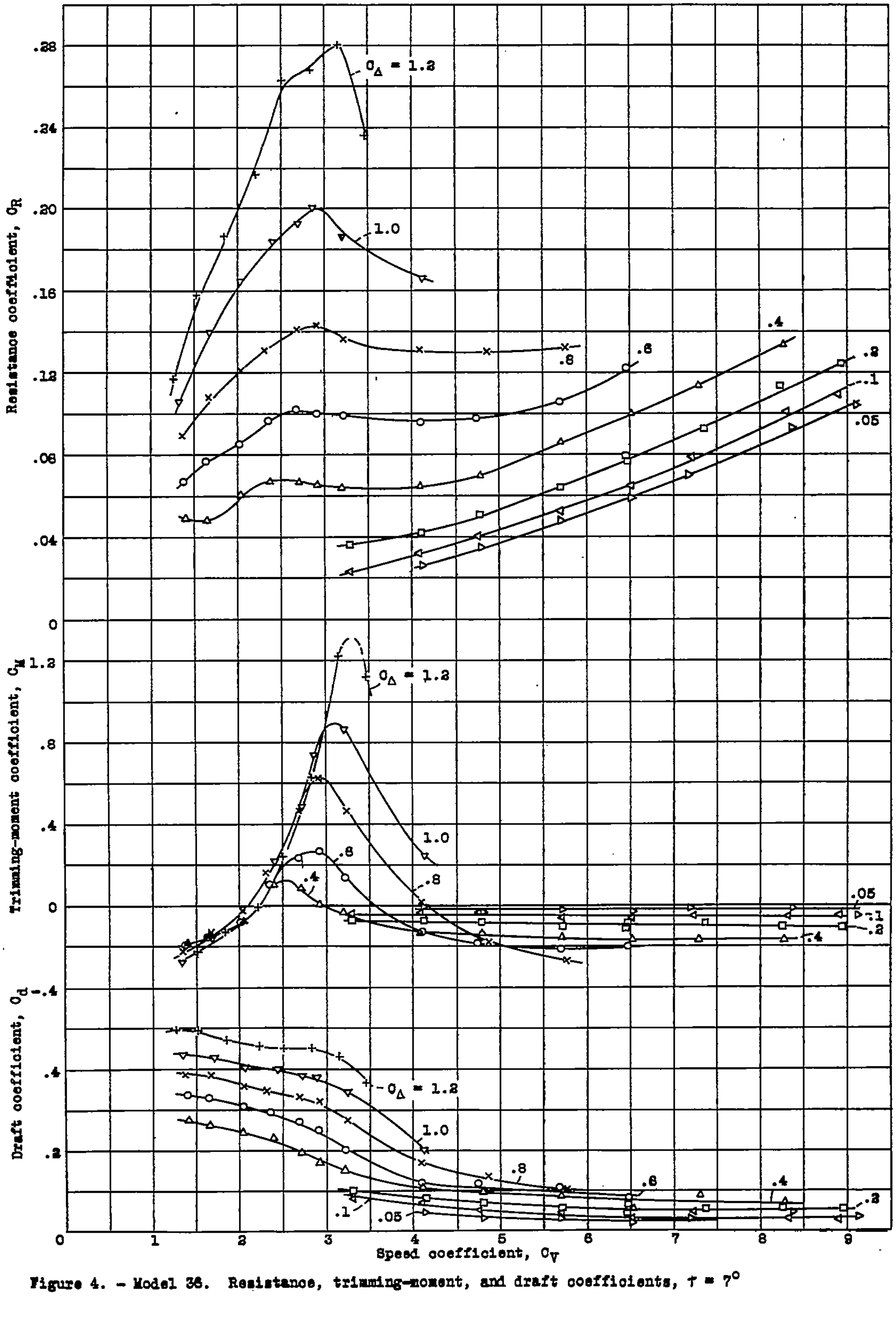

Figure 4. - Model 36. Resistance, trimming-moment, and draft coefficients, τ = 7°

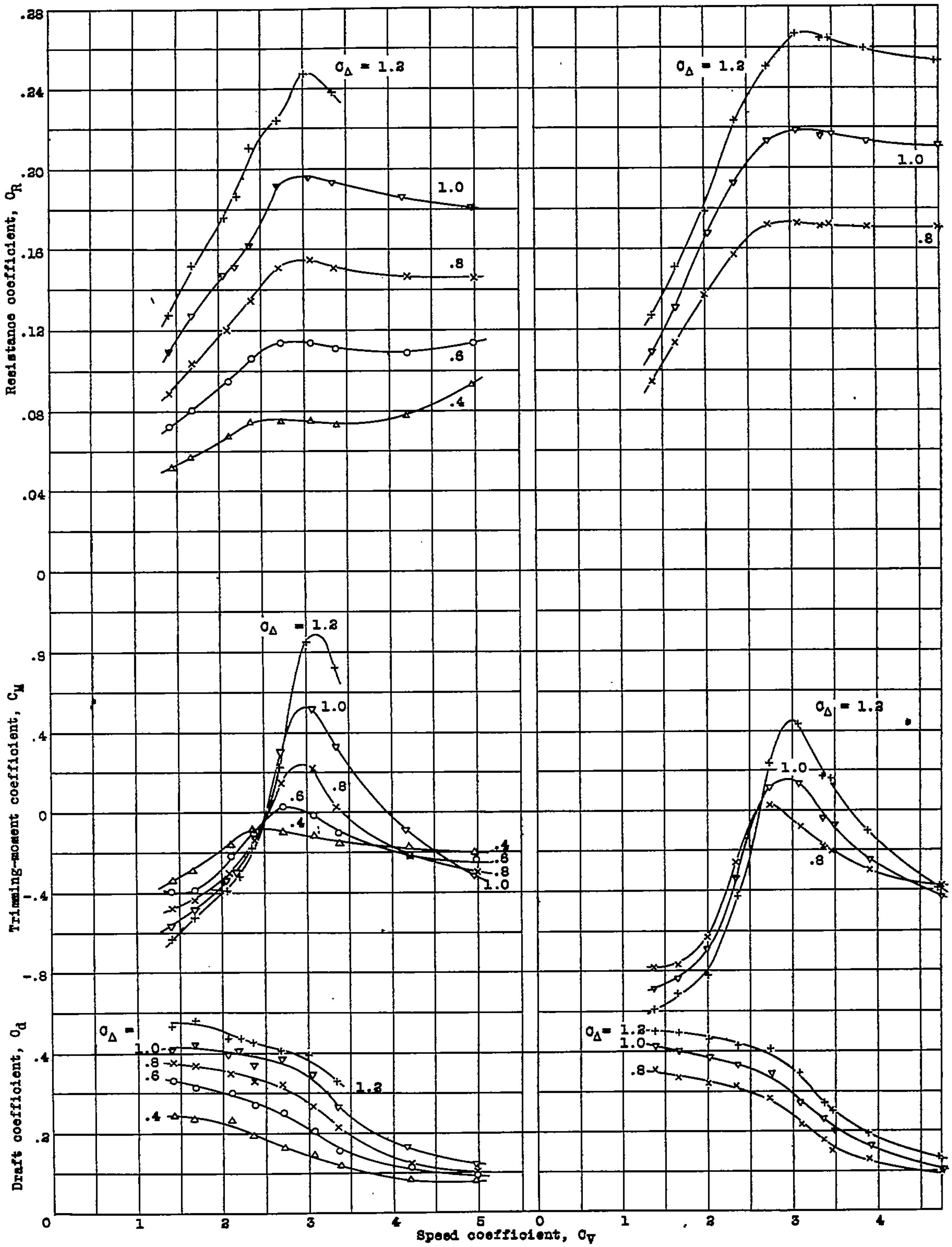

Figure 5.- Model 36. Resistance, trimming-moment, and draft coefficients. $\tau = 9°$

Figure 6. - Model 36. Resistance, trimming-moment, and draft coefficients. $\tau = 11°$

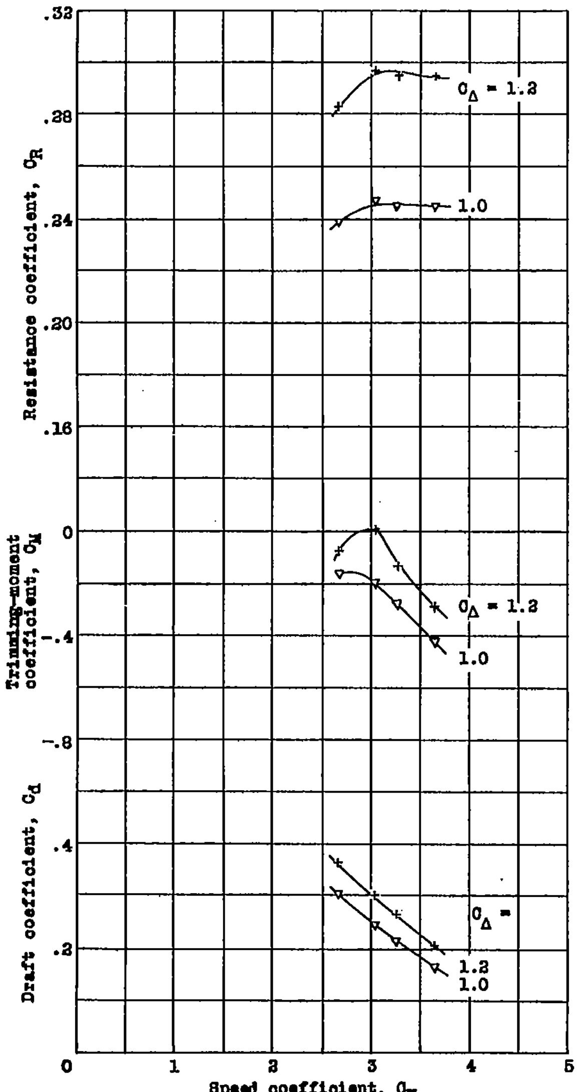

Figure 7.- Model 36. Resistance, trimming-moment, and draft coefficients. $\tau = 13°$

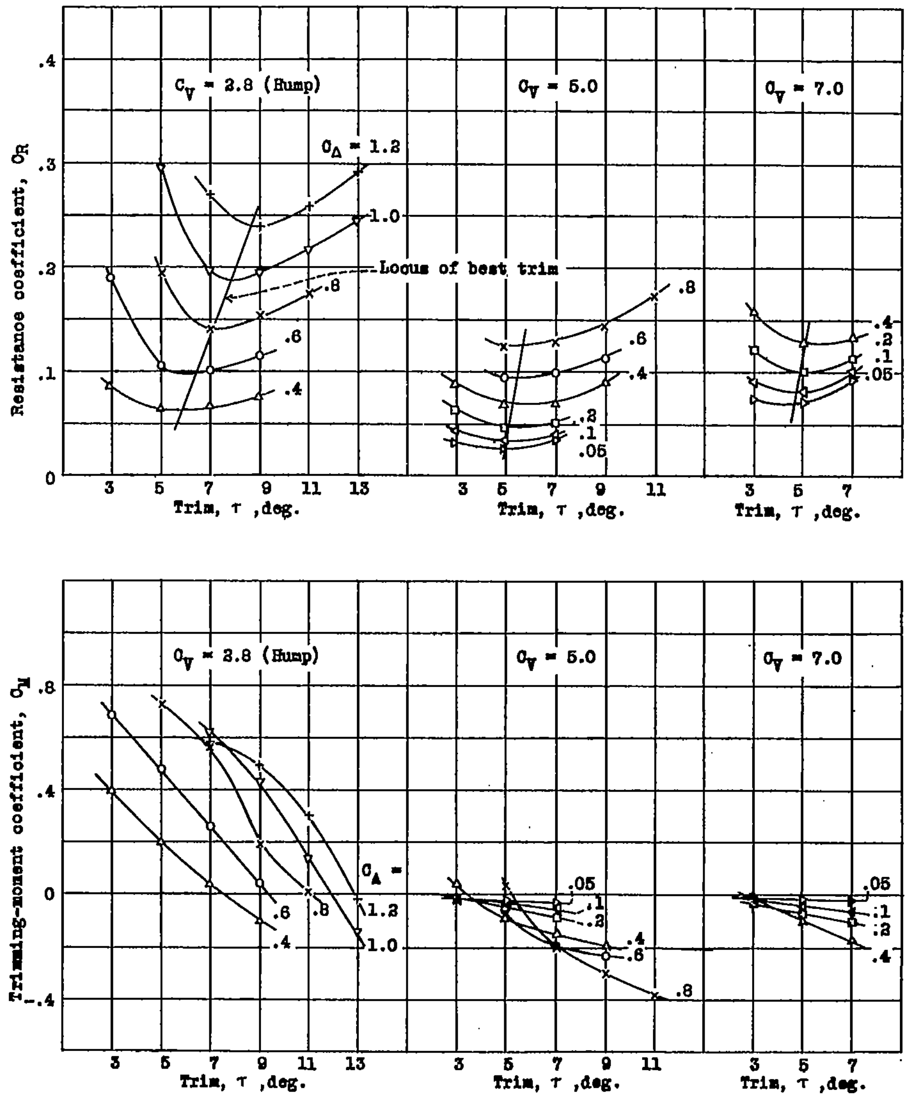

Figure 8.- Model 36. Variation of C_M and C_R with trim, at selected speed coefficients.

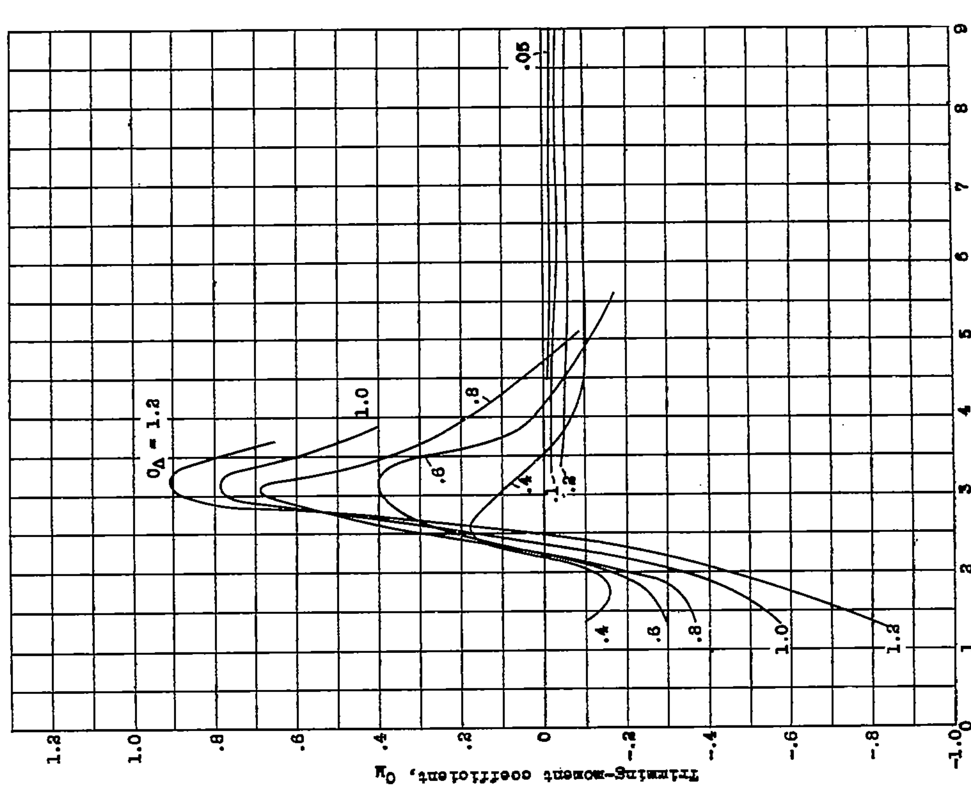

Figure 10. - Model 36. Variation of C_M with C_V at best trim, with center of moments 10 inches forward of the step.

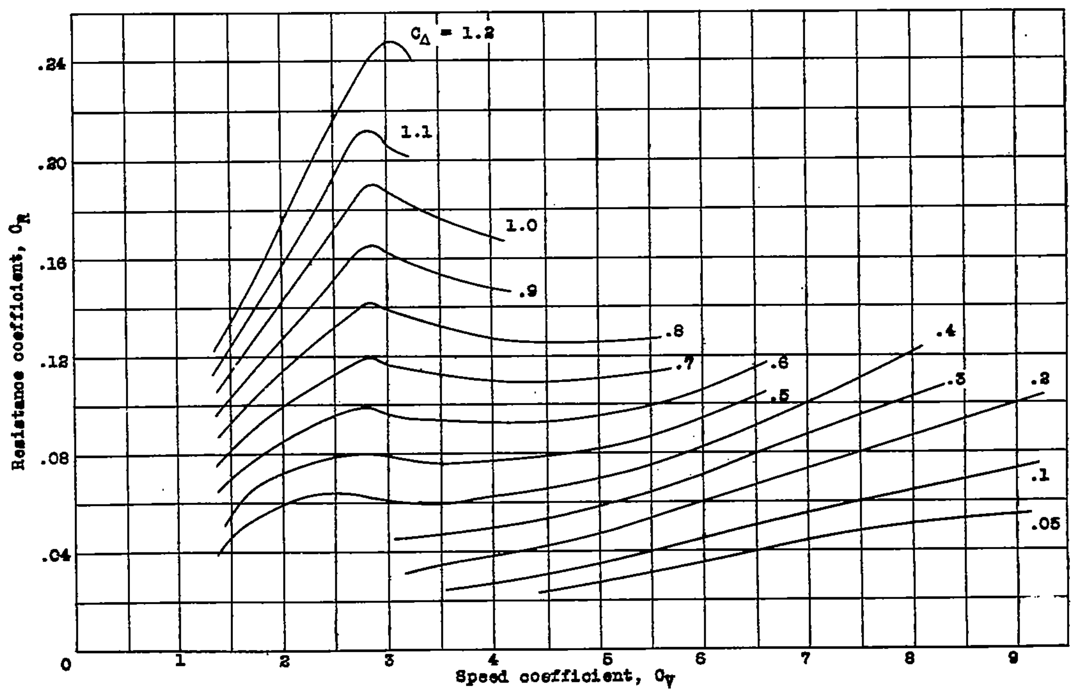

Figure 9. - Model 36. Variation of C_R with C_V at best trim.

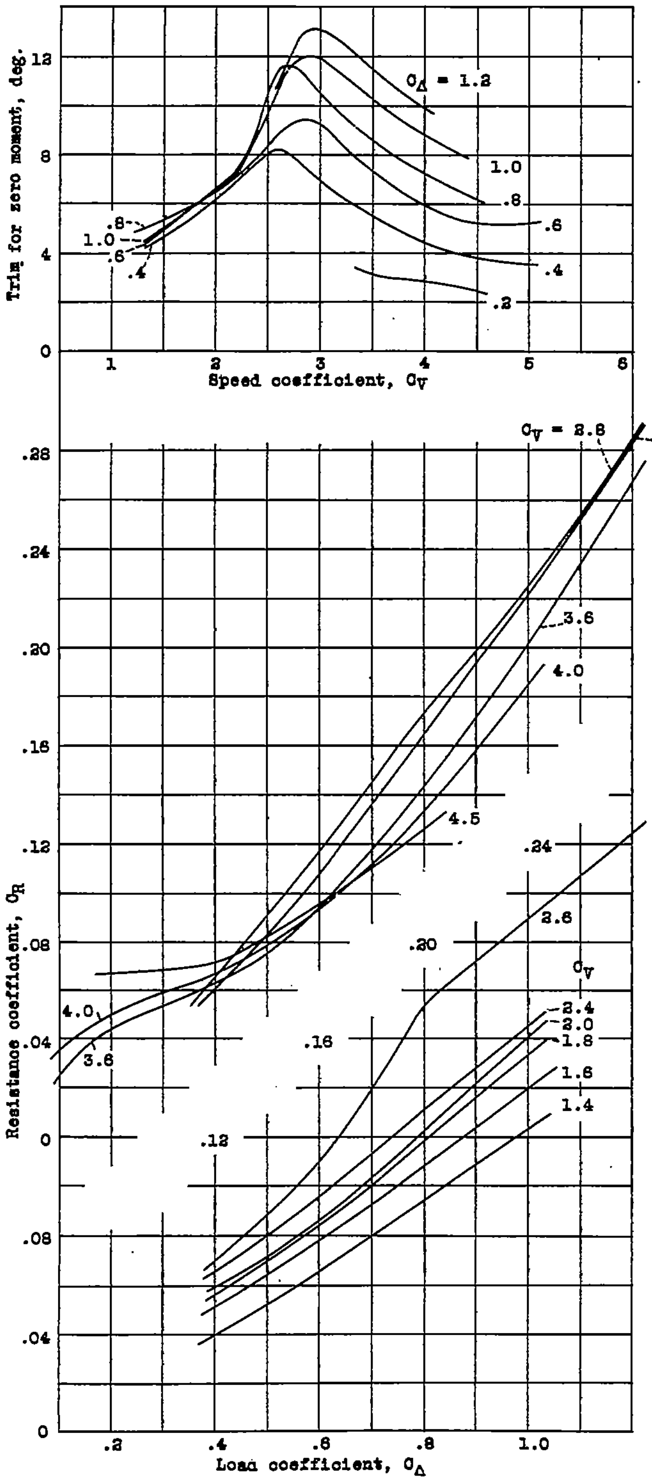

Figure 12.- Model 36. Chart for determining resistance and trim at zero trimming moment. Center of gravity 10 inches forward of the step.

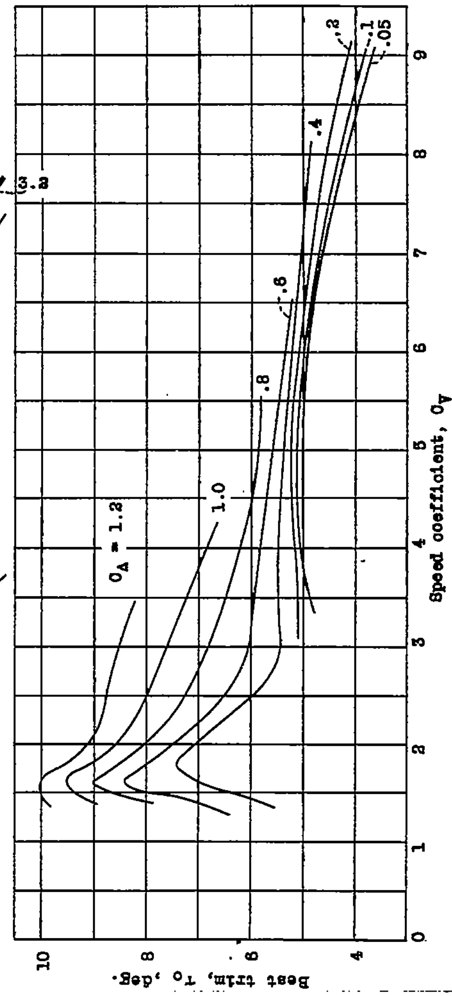

Figure 11. - Model 36. Variation of τ_o with C_V

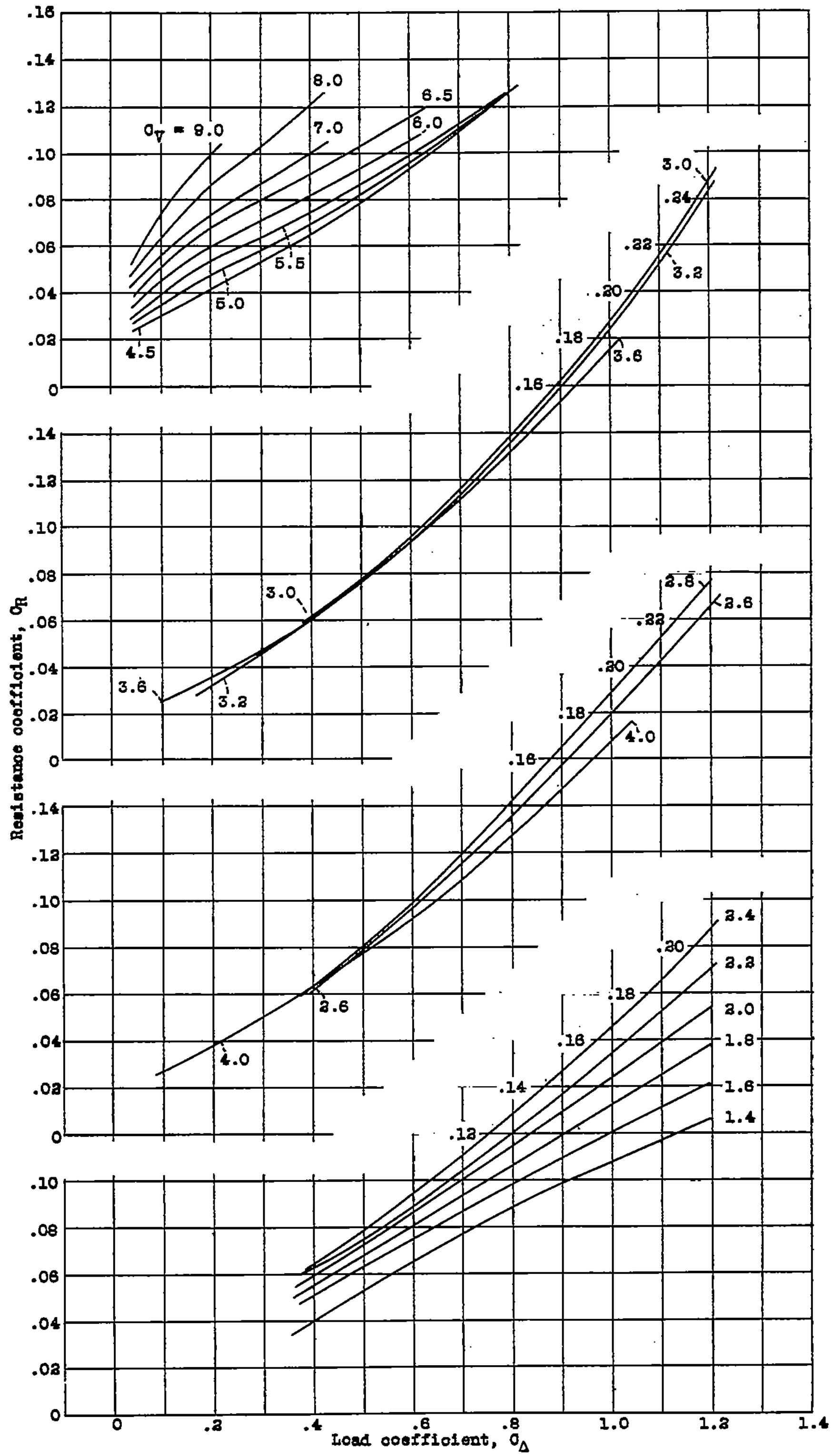

Figure 13. - Model 36. Chart for determining resistance at best trim.

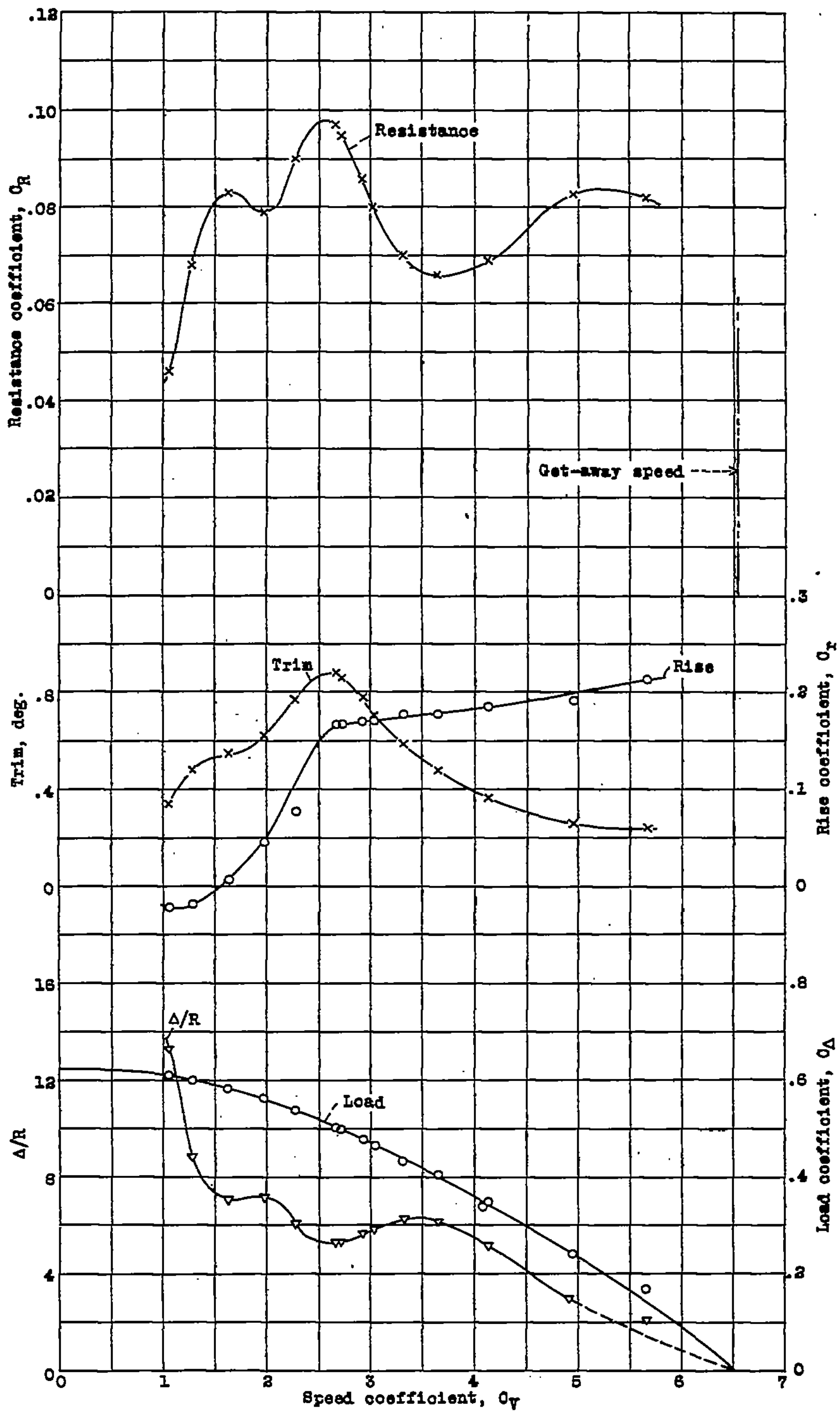

Figure 14. - Model 36. Results of specific test at 62.7 pounds initial load, center of gravity 10 inches forward of the step.

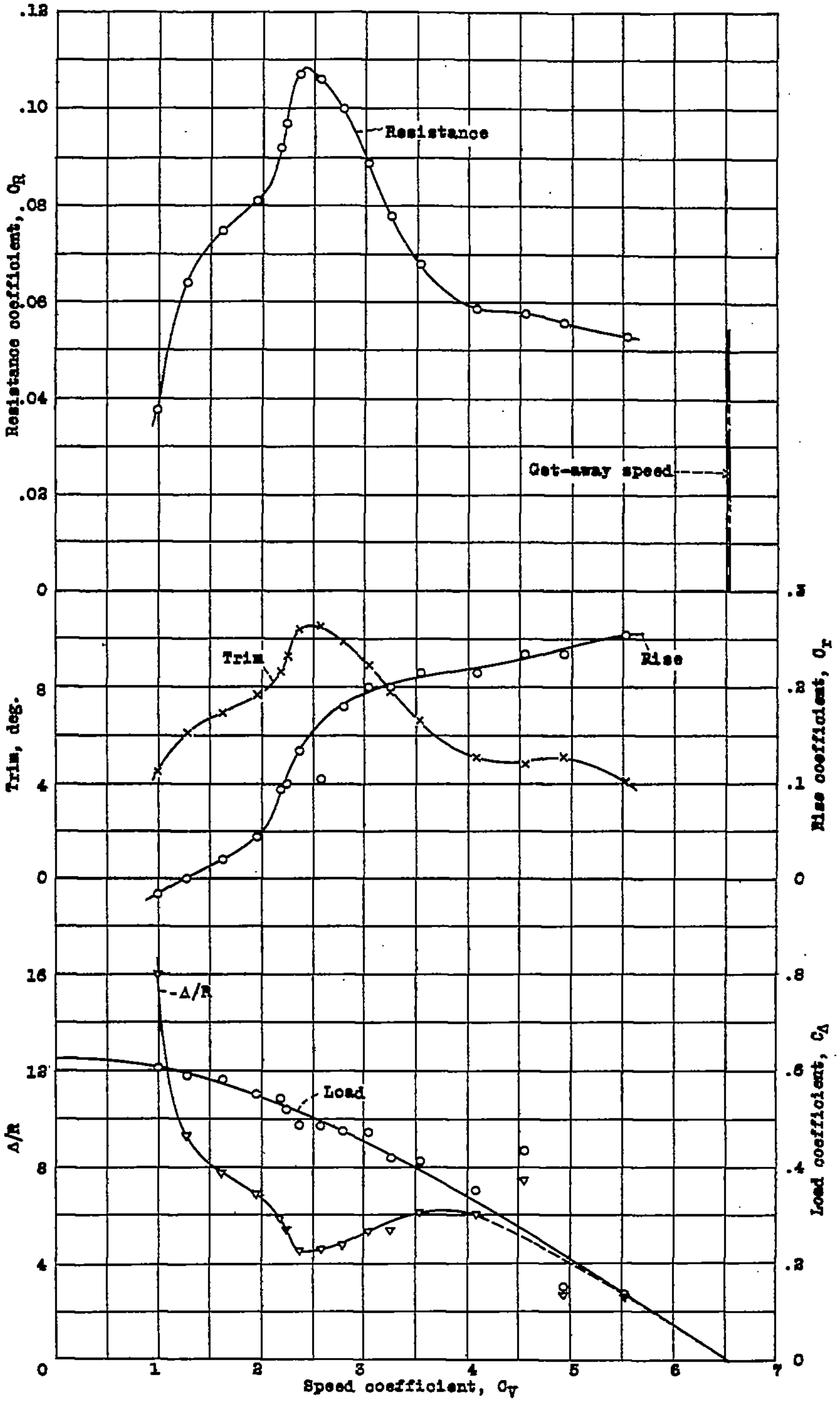

Figure 15. - Model 36. Results of specific test at 62.7 pounds initial load, center of gravity 6⅞ inches forward of the step.

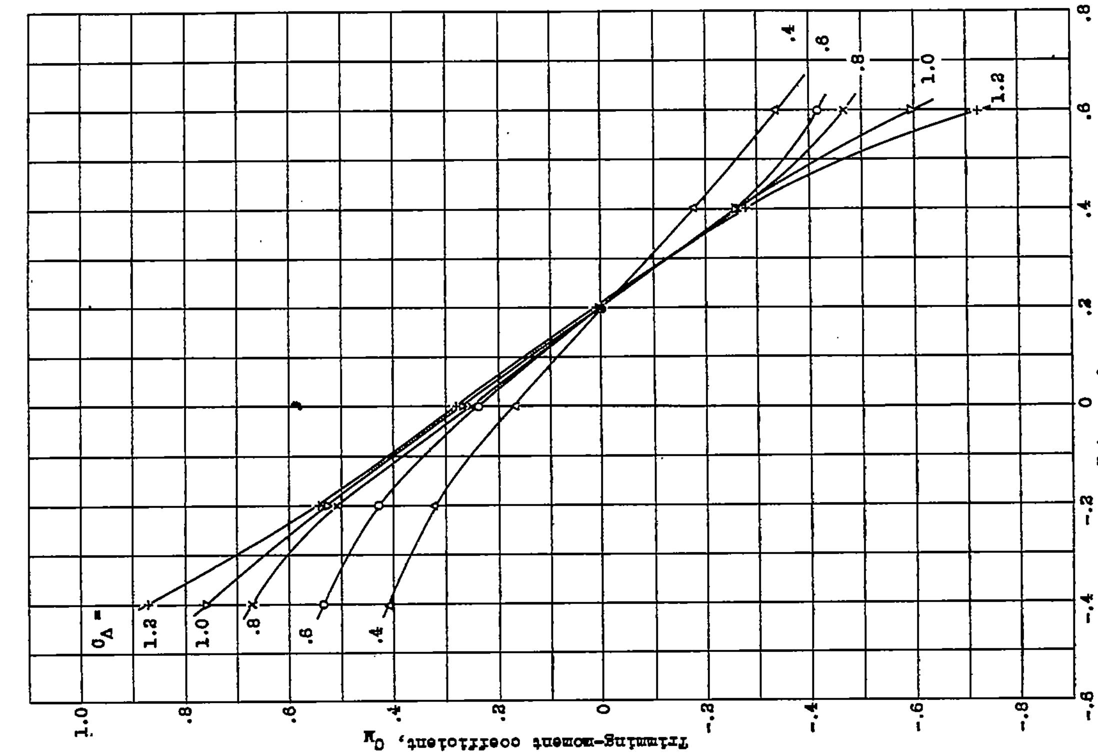

Figure 17. - Trimming-moment coefficients at rest, with center of moments 10 inches forward of step. Model 36.

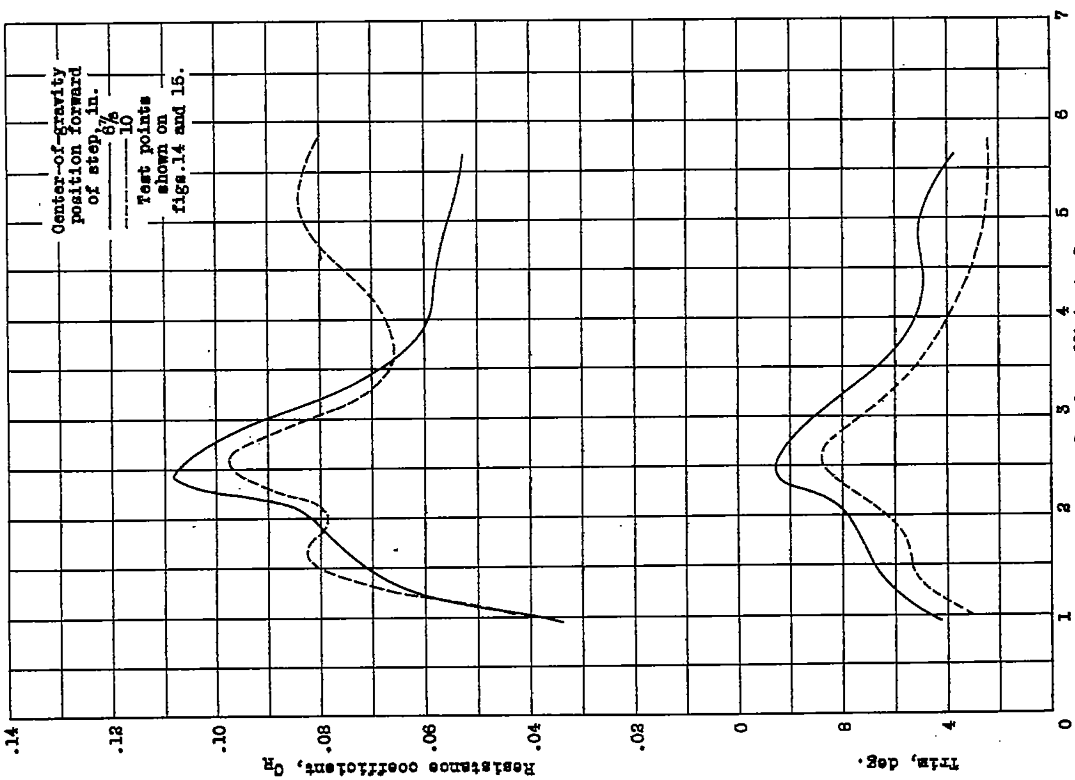

Figure 16. - Model 36. Effect of center-of-gravity position upon resistance and trim.

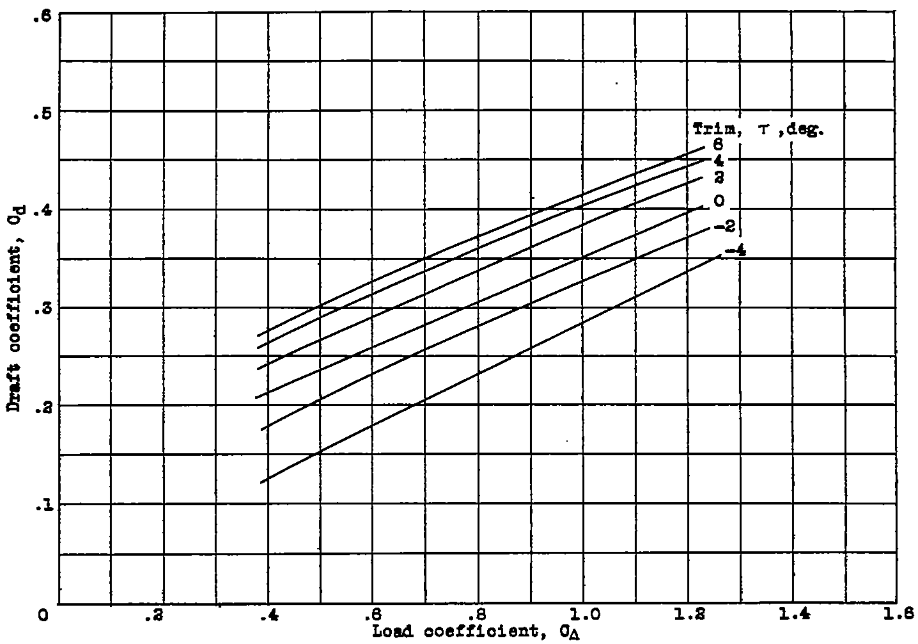

Figure 18. - Model 36. Draft coefficients at rest.

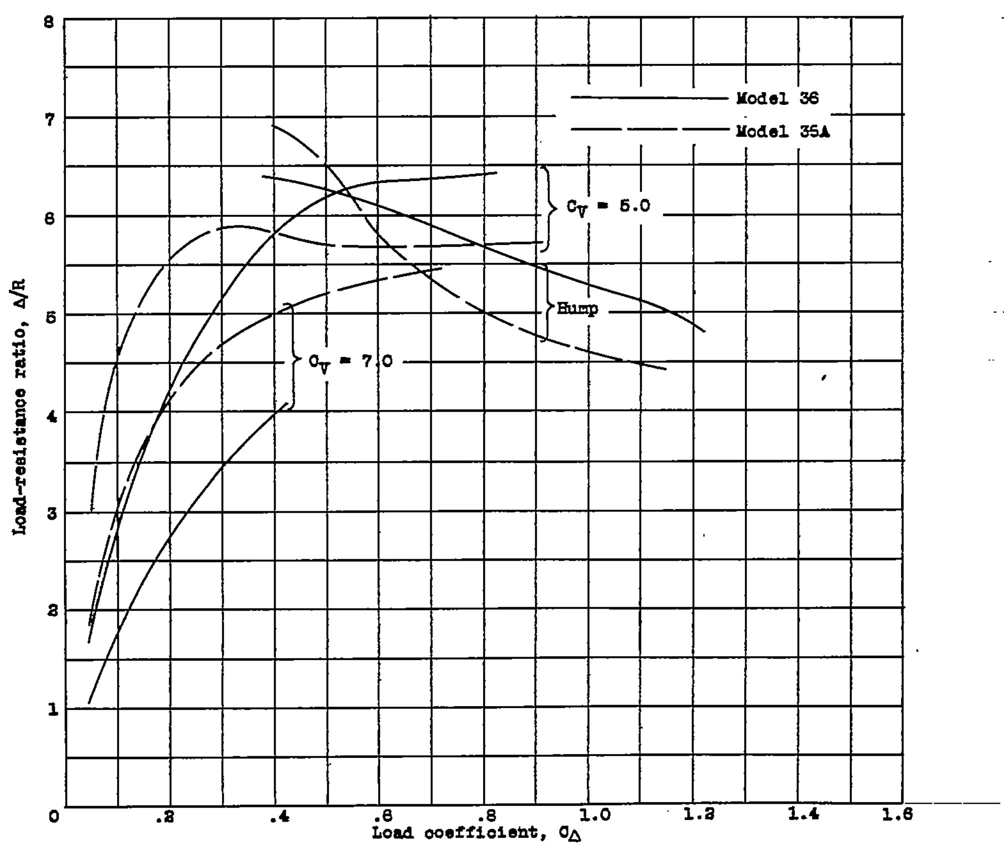

Figure 22. Model 36. Comparison of load-resistance ratios of models 36 and 35A, at best trim.

(a) (b)

$C_V = 2.3$, $\tau = 7.7^\circ$, $C_\Delta = 0.54$.

(c) (d)

$C_V = 2.7$, $\tau = 8.6^\circ$, $C_\Delta = 0.50$.

(e) (f)

$C_V = 2.9$, $\tau = 7.8^\circ$, $C_\Delta = 0.48$.

Figure 19. - Model 36. Spray photographs, free-to-trim. Center of gravity 10 inches forward of the step.

(a) (b)
$C_V = 2.73$, $\tau = 11^{\circ}$, $C_{\Delta} = 1.2$.

(c) (d)
$C_V = 2.71$, $\tau = 7^{\circ}$, $C_{\Delta} = 1.0$.

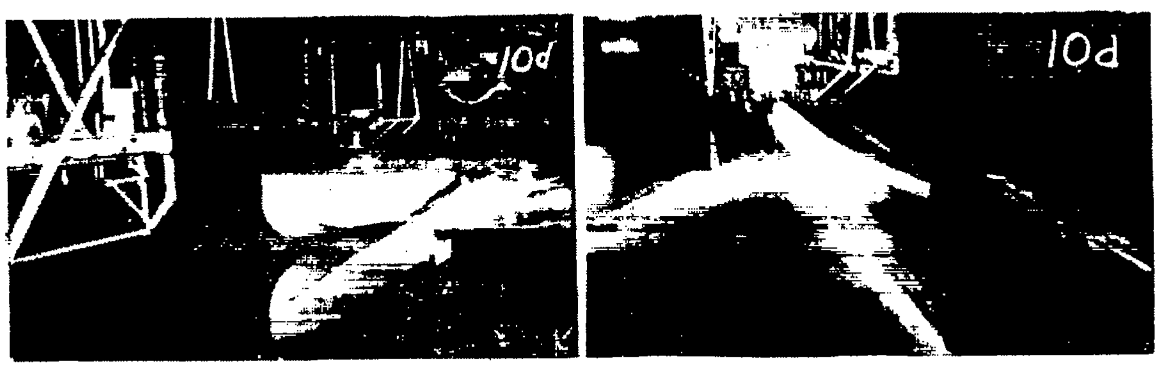

(e) (f)
$C_V = 4.22$, $\tau = 5^{\circ}$, $C_{\Delta} = 0.4$

Figure 20. - Model 36. Spray photographs, fixed trim

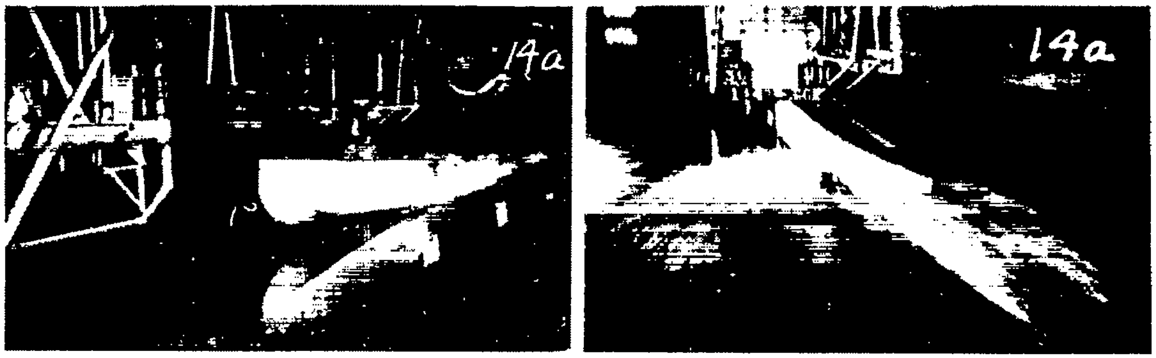

(a)   (b)

$C_V = 5.74$, $\tau = 5^o$, $C_\Delta = 0.1$.

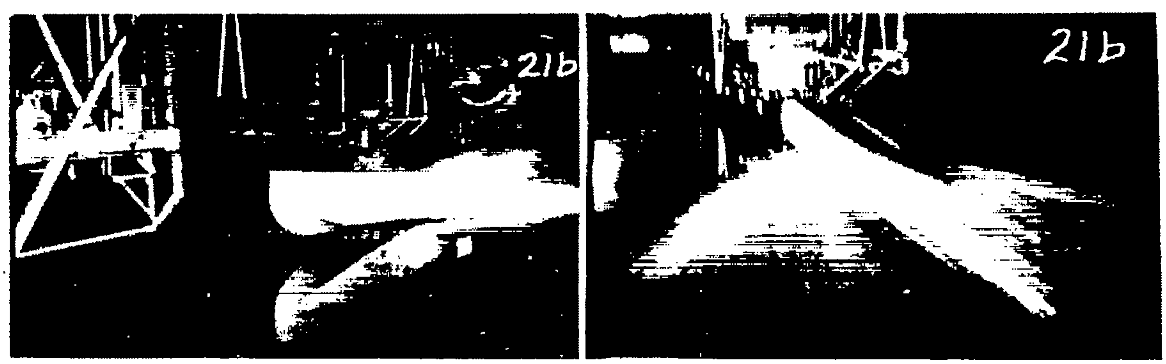

(c)   (d)

$C_V = 5.74$, $\tau = 5^o$, $C_\Delta = 0.4$.

Figure 21. - Model 36. Spray photographs, fixed trim, high speeds.